25th ABCM International Congress of Mechanical Engineering
October 20-25, 2019, Uberlândia, MG, Brazil

COB-2019-1503
ISHM BASED APPROACH FOR FAULT DETECTION IN A ROTATING MACHINE WITH A COMPOSITE SHAFT

Marcela Andréa Teodoro Sousa
Karina Mayumi Tsuruta
Lucas A. A. Rocha
Roberto Mendes Finzi Neto
Aldemir Ap. Cavalini Jr.
Valder Steffen Jr.
LMEst - Structural Mechanics Laboratory, Federal University of Uberlândia, School of Mechanical Engineering, Av. João Naves de Ávila, 2121, Uberlândia, MG, 38408-196, Brazil
marcelateodoro@ufu.br, karinamt@ufu.br, lucasaarocha@ufu.br, finzi@ufu.br, aacjunior@ufu.br , vsteffen@ufu.br

Abstract. *Composite materials shafts have been showing promising results when applied to rotating machines due to its low weight/strength ratio and good fatigue resistance. Despite the advantages in comparison to more traditional materials, composites present different types of damage that are difficult to detect. Therefore, it is necessary to use monitoring techniques to detect incipient damages and prevent failure. So, this work evaluates the structural health monitoring (SHM) method based on electromechanical impedance (ISHM) applied in a rotating machine with composite shaft. This methodology uses the piezoelectric material as sensor and actuator to detect damage. Such approach monitors changes in the electric impedance of piezoelectric transducers that are bonded to the host structure. Normally the evaluation of the impedance responses is performed by using damage metrics, which permit to quantify the influence of damage. This is possible since the sensor electrical impedance is directly related to the mechanical impedance of the structure. For this investigation, two sensors (each one with four piezoelectric patches connected in parallel) were attached on composite shaft. To simulate the damage condition, a nut was attached in different positions on the shaft, also in order to increase the robustness of the ISHM technique, the effects of rotation speed of the rotor and temperature variation were evaluated. Additionally, a data normalization based on hybrid optimization method associated with a given damage metrics is used to minimize theses influences.*

Keywords: *structural health monitoring, rotating machine, electromechanical impedance method, composite shaft.*

1. INTRODUCTION

Over the past decades composite materials have been replacing traditional materials due to characteristics such as high strength-to-weight ratio, high specific stiffness and long fatigue life (Alwan et al., 2010). This type of material offers the possibility of obtaining a desired characteristic by changing: the material used, the number of layers and orientation of each layer (Mendonça et al., 2017). In rotating machinery, the composite materials are replacing metal in automotive drive shafts, helicopter rotors and in aircrafts actuation systems (Sino et al, 2008 and Cavalini Jr. et al., 2017).
Despite the advantages of this material, composite materials have more complex damage mechanisms than traditional materials, due the damage is difficult to detect in early stages and even lead to failure (Wilson et al., 2018). Therefore, it is important to develop and improve structural health monitoring (SHM) techniques that enable online damage detection and assessment. One SHM technique that has been widely studied and shows promising results is the electromechanical impedance method, initially proposed by Liang et al. (1994). This method uses the direct and inverse effect of the piezoelectric materials, in the direct effect (sensor), an electric charge is produced when the piezoelectric transducer is mechanically strained and in the inverse effect (actuator), a piezoelectric patch deforms when an electrical potential is applied. In the ISHM technique measures the electric impedance of a piezoelectric transducer bonded on/into the host structure, and this signature is direct related to the dynamic response of the structure, therefore, when damage occurs, the electrical signal measured by impedance sensors will change. A particular damage metric is normally used to quantify the severity of the failure by means of statistical equations that represent the changes between a baseline (pristine) condition and another test measurement (Park and Inman, 2005).

Several studies show that the ISHM method can be successfully applied to composite structures, Tsuruta (2008) evaluate the method to detect damages with low-energy impact on CFRP plates. Schwankl et al. (2012) developed a finite element model and experimental for an aluminum disc with SHM technique, then applied this experimental methodology on a composite stiffened panel. Na and Lee (2012) developed a technique to eliminate the trial and error method to

determine the frequency band to detect damages on a glass-epoxy composite plate with large surface areas. Selva et al. (2013) used artificial neural networks to predict the in-plane localization of damage detected using ISHM method for aeronautical composite plates. Wandowski et al. (2016) studied using ISHM technique to detect delamination in large plates of composite materials, furthermore, studied the influence of the temperature and used signal-cross-correlation to compensate this influence in the impedance signatures. As the Temperature effects are known to cause a frequency (horizontal) and amplitude (vertical) shift in the impedance signatures. The compensation technique improved the sensitivity of the method to damage, but it can only be done in small frequency ranges since the frequency shift is frequency dependent (Park et al, 2015).

In relation to ISHM methods applied on rotating machines, few studies have been founded. Cavalini Jr et al. (2014) evaluated the application of impedance technique in rotating systems, acquiring the impedance signal with the rotor both at rest and in movement for detection of incipient damages in rotating shafts. In this study, the PZT patches were mounted on the shaft and on one of the discs pf the rotor. Tsuruta et al. (2017) applied a hybrid optimization technique to minimize external influences such as temperature and dynamic loads in the use of ISHM on a metal shaft, stablishing a threshold based on Statistical Process Control method to estimate the performance of each sensor. So, the object of this work is to analyze the use of the ISHM method to detect incipient damage in a carbon fiber reinforced polymer hollow shaft, considering different rotating speeds and different positions of the damage.

2. THE ELECTROMECHANICAL IMPEDANCE METHOD

The ISHM technique uses piezoelectric transducers coupled to the host structure, using their sensor and actuator properties to detect damage, monitoring changes on the stiffness, damping, and mass of the structure, as based on the electromechanical coupling property of the intelligent structure. For this aim, an electrical impedance measurement is acquired from the piezoelectric transducer, as due to the difficulty of obtaining the mechanical impedance of the structure. Considering that the properties of the PZT patch (Lead Zirconate Titanate) do not vary over time, changes in the electrical impedance will be directly related to changes in the mechanical impedance, which is affected by the presence of damage (Park et al, 2006). Figure 1 shows a *single-degree-of-freedom* (DOF) electromechanical model proposed by Park et al. (2006) that describes the measurement process. The piezoelectric transducer is bonded directly with a high-strength adhesive on the surface of the structure to ensure better electromechanical coupling (Peairs, 2006). The dynamic properties of the monitored structure are represented by a mass (M), a stiffness (K) and a damping factor (C). So, the piezoelectric transducer is excited by a sinusoidal voltage source $V_i(\omega)$ with amplitude V and angular frequency ω. Using the actuator effect, the piezoelectric transducer applies a force on the host structure; in response, it returns an induced strain. Through the sensor effect, this induced strain generates an output current $I_o(\omega)$ with amplitude i and phase ϕ. The mechanical impedance $Z_m(\omega)$ of the monitored structure is given by the relation between the force applied $F(\omega)$ to the structure and the speed $\dot{X}(\omega)$ developed. Making an analogy with an electric circuit, the force and speed correspond to a voltage and output current, respectively, resulting the electrical impedance $Z_e(\omega)$. This function is measured using an appropriate measurement device (normally, the inverse of the impedance is analyzed, the admittance).

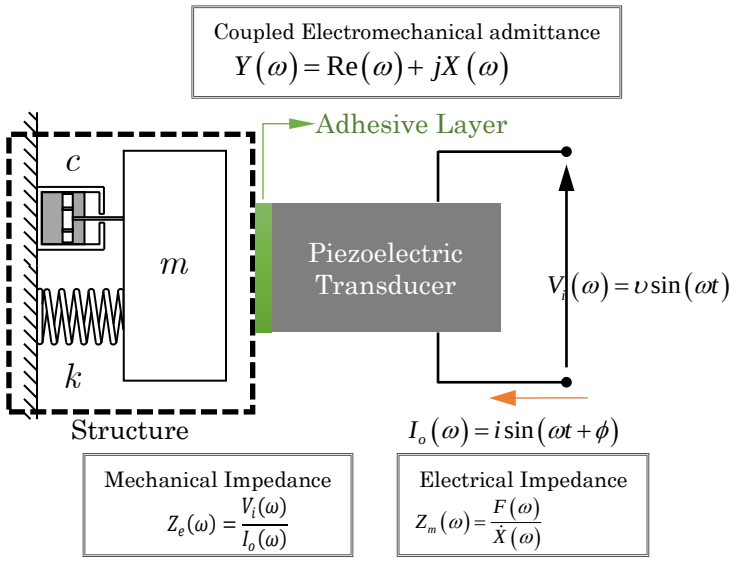

Figure 1 – A single DOF Electromechanical Model of the impedance-based structural health monitoring method (Park et al, 2006).

Equation 1 shows the frequency-dependent electrical admittance. This is the solution of the wave equation for the piezoelectric transducer connected to the structure (Park et al., 2006). Based on the system shown in Fig. 1, the *admittance* $Y(\omega)$ (inverse of impedance) of the piezoelectric transducer is a combined function involving the mechanical impedance of the PZT actuator $Z_a(\omega)$ and the structure $Z_s(\omega)$, according to:

$$Y(\omega) = R(\omega) + jX(\omega) = \frac{I_o(\omega)}{V_i(\omega)} = j\omega \frac{b_a l_a}{h_a}\left(\bar{\varepsilon}_{33}^{T}(1 - j\delta) - \frac{Z_s(\omega)}{Z_s(\omega) + Z_a(\omega)} d_{31}^2 \hat{Y}_{11}^{E}\right) \quad (1)$$

where $R(\omega)$ and $X(\omega)$ are the real part and imaginary part of the electromechanical admittance, respectively; j is the imaginary unit, ω is the angular frequency; b_a, l_a, h_a is the width, length and thickness of the piezoelectric transducer; $\bar{\varepsilon}_{33}^{T}$is the dielectric constant at zero stress, δ is the dielectric loss tangent to the piezoelectric transducer; d_{31}^2 is the piezoelectric coupling constant at zero electric field; $\hat{Y}_{11}^{E}$is the complex Young's modulus of the PZT patch with zero electric field. The impedance is a frequency dependent complex function. To obtain the electrical impedance, both the direct and inverse effects of the piezoelectric transducer are used. The direct effect (or sensor effect) is characterized by producing a voltage when the piezoelectric transducer is mechanically deformed in the elastic phase, and the inverse effect (or actuator effect) appears as a piezoelectric ceramic patch is subjected to a voltage, resulting a mechanical deformation (Peairs, 2006).

Frequency band for the ISHM method is normally chosen by a trial and error method considering the structure characteristics, according to the work developed by (Peairs, 2006). It has been found that a frequency range with a high mode density exhibits a higher sensitivity since it generally covers more structural dynamic information (Peairs, 2006).

The detection and evaluation of the structure integrity is based on the comparison between the real part of the impedance signatures acquired from both the healthy and damaged (or unknown condition) structure. A visual examination of the signals is not enough for evaluation, since it gives only a qualitative comparison. Consequently, it is necessary to use an adequate metrics for defining quantitative criteria. Thus, damage metrics (DM) are employed, i.e., scalar parameters are properly defined so that they can numerically represent the difference between the two signals (without and with damage). According to Palomino (2008) the most used metric in this case is the root mean square deviation (RMSD), defined by Eq. (2), where $Z_{1,i}$ and $Z_{2,i}$ are the impedance functions measured for the healthy and damaged structure, respectively, and n is the number of frequencies in the observation band. This metric will be used to analyze the results of this work.

$$RMSD = \sqrt{\sum_{i=1}^{n}\left\{\frac{\left[\mathrm{Re}(Z_{1,i}) - \mathrm{Re}(Z_{2,i})\right]^2}{n}\right\}} \quad (2)$$

3. OPTIMIZATION PROCEDURE

Temperature variation effects are known to cause horizontal (frequency) and vertical (amplitude) shifts in impedance signatures. A review of temperature variation effects and temperature methods can be found in Rabelo (2016).

Figure 2 shows a flowchart to illustrate the proposed temperature compensation methodology. The method starts by obtaining the impedance signatures of the healthy analyzed system ($Imp_{baseline}$; temperature $T_{baseline}$). The impedance signatures of the system for an unknown condition ($Imp_{unknown}$; temperature $T_{unknown} \neq T_{baseline}$) are also required, so that the optimizer is responsible for shifting their effective frequency and amplitude. The $Imp_{unknown}$ signatures are compared with the $Imp_{baseline}$ ones by means of a given objective function, i.e., a damage metric.

In Fig. 2, if the procedure converges to a minimum value of the objective function, the effects of temperature variation are compensated through the frequency shift and vertical shift design variables. If this is not the case, the optimization procedure continues the search with new frequency and amplitude shifts. The optimization process continues iteratively until convergence is assured, which can lead to temperature compensation (if the objective function is close to zero) or a damage indication associated with temperature compensation.

The present contribution, a hybrid optimization technique is primarily devoted to minimizing temperature during the impedance measurement process. Also, this optimization process was used to test its effectiveness in minimizing the influence of the external excitation on the impedance signatures. The following section describes the hybrid optimization algorithm.

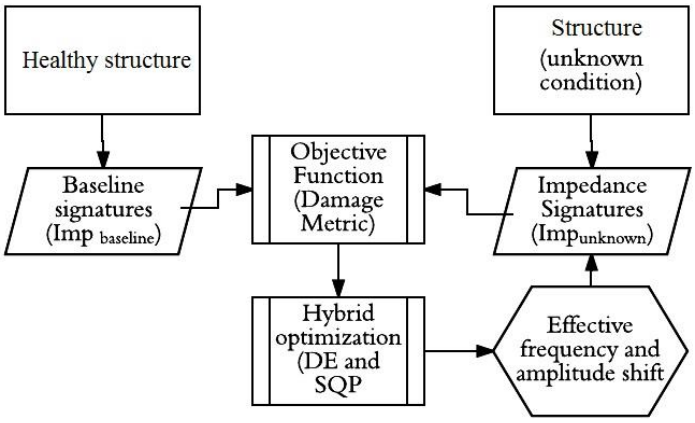

Figure 2 – Proposed noise compensation flowchart.

The proposed temperature compensation technique is based on the solution of a typical inverse problem, in which the optimal effective frequency and amplitude shifts are determined by minimizing the damage metric associated with two impedance signatures (i.e., one of the signatures corresponds to the baseline). Thus, the evolutionary technique known as Differential Evolution (DE) (Price et al, 2005) is devoted to the global search for the optimum (i.e., the effective frequency and amplitude shifts). It is worth mentioning that the DE algorithm must be performed n times to avoid local minima. The best result obtained by DE is then used as a starting point for the classical direct method Sequential Quadratic Programming (SQP) to obtain the local and refined optimal solution.

The DE algorithm is an optimization technique that belongs to the family of evolutionary computation, which differs from other evolutionary algorithms in the mutation and recombination schemes. DE executes its mutation operation by adding a weighted difference vector between two individuals to a third one. Then, the mutated individuals will perform discrete crossover and greedy selection with the corresponding individuals from the last generation to produce the offspring. The key control parameters for DE are the population size (NP), the crossover constant (CR), and the associated weight (F).

In the work developed by Storn and Price (1995), simple rules are given for choosing the key parameters of DE for general applications. Normally, NP should be about 5 to 10 times the dimension of the problem (i.e., the number of design variables). As for F, it lies in the range between 0.4 and 1.0. Initially, F = 0.5 can be tried, and then F and/or NP can be increased if the population converges prematurely. In Price et al. (2005) various mutation schemes where proposed for the generation of new candidate solutions by combining the vectors that are randomly chosen from the current population. In the applications of this paper, the rand / 1 scheme was used.

4. STATISTICAL THRESHOLD DETERMINATION

A reliable SHM system should be able to provide diagnosis with a pre-configured level of confidence based on the pristine conditions of the host structure. In many experimental tests, it is recommended that the measured data is cleansed to eliminate spurious or degraded signals that might have resulted from acquisitions and processes associated with excessive noise, signal dropouts, or even an external cause such as power failure (Rabelo et al., 2016).

4.1 Statistical Threshold Determination

The concepts behind Statistical Process Control allow to establish limits in a control chart so that a threshold can be established using the upper control limit. These limits can be defined so that 95.45 % or 99.73 % of data from a normally distributed population remains, if these control limits are established as expressed in Eq. (3).

$$\bar{x} \pm 2s \quad for \ \ 95.45\% \ \ confidence$$
$$\bar{x} \pm 3s \quad for \ \ 99.73\% \ \ confidence \tag{3}$$

where $\bar{x}$ is the sample mean and s is the sample standard deviation (Rabelo et al., 2016).

5. METHODOLOGY

Figure 3 shows the test rig used for evaluating the ISHM technique to detect damage on a rotating machine with CFRP shaft. This rotor is composed by a flexible composite shaft (907 mm length, 18 mm width and 5.2 mm thickness) and two rigid discs (both with 202.7 mm diameter and 20 mm thickness). The shaft is supported by two roller bearings.

The system is driven by a direct current (DC) electric motor. A flexible shaft coupling (Rocom Corp® model DTOOO175) was used to minimize the interaction between the electric motor and the shaft.

Figure 4 shows a schematic drawing of the rotor with the main dimensions between the rotor parts, as well the position of the piezoelectric transducers and damages on the composite shaft. Two PZT patches were attached on the shaft, each one is composted by 4 piezoelectric transduces (10 mm length, 3 mm width, and 1 mm thickness) electrically connected in parallel as showed in the Figure 5 (a), named PZT#1 (75 mm from the Disc-1) and PZT#2 (65 mm to the right of the first disc. The frequency range was determined experimentally based on the density of peaks: [80 – 110] kHz for all the PZT patches.

A slip ring (Michigan Scientific's S-Series Slip Ring - C556019) was used on the rotor under operation in order to measure the electrical signals from the PZT patches (Fig.5 (b)). This device can transfer electrical signals from fixed to rotating parts (and vice versa) with low noise interference, even for the rotor operating at high speeds. According to the manufacturers, the device can transfer electrical signals from accelerometers with the rotor operating in a range of 0 - 12,000 RPM. Figure 5 (c) shows the impedance measurement system.

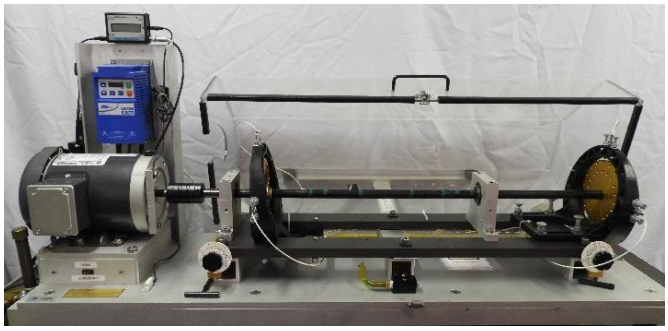

Figure 3 – Test rig used for evaluating the ISHM technique.

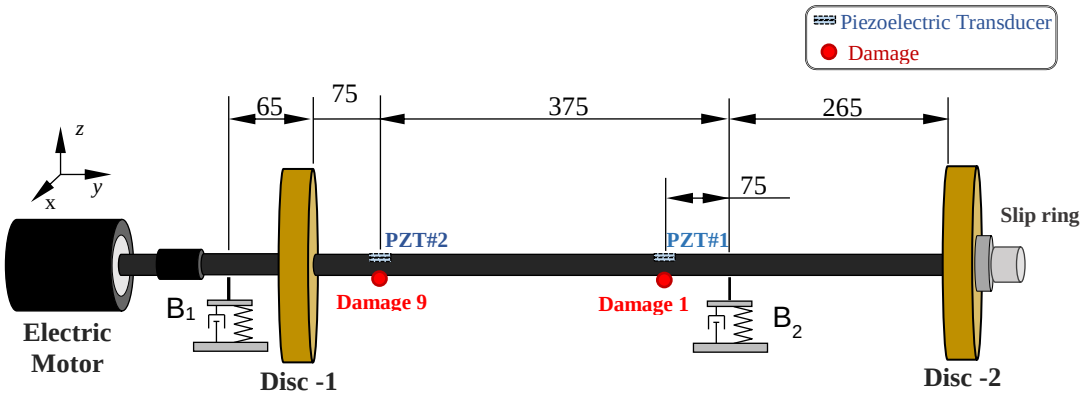

Figure 4 - Scheme of the test rig used with main dimensions.

For the condition that the rotor was stationary the impedance signatures were measured as showed in Table 1, damage was simulated, a nut with 0,45 g (Fig. 5(d)) was bonded on the shaft in different positions. Also, the impedance signals were obtained under operation on three different speeds (600 RPM, 900RPM and 1200 RPM). For each condition of the experiment, 30 measurements were acquired, with 3000 points and 256 averages each. The impedance was measured by an impedance measurement system (Finzi Neto et al.,2011).

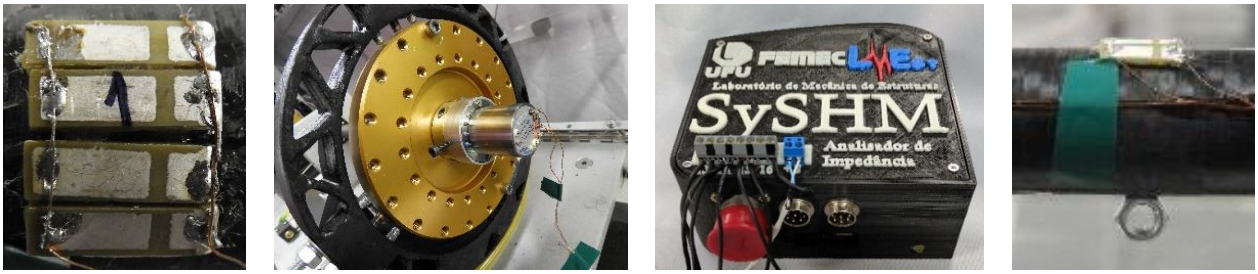

(a) (b) (c) (d)

Figure 5 - (a) Piezoelectric transducer; (b) Slip ring attached to the disc-2; (c) Impedance measurement system, (d) Nut bonded on the composite shaft to simulate damage.

Table 1. Experimental configuration adopted to obtain the rotor impedance signatures (Rotor OFF).

	Run	Structure condition	Damage	Distance from PZT#1 (Direction Disc-1)	Nomenclature /Graphic
PZT#1	1	Baseline	-	-	BL
	2	Damage 1	Yes	Opposed	D1
	3	Damage 2	Yes	10 mm	D2
	4	Damage 3	Yes	20 mm	D3
	5	Damage 4	Yes	30 mm	D4
	6	Damage 5	Yes	40 mm	D5
	7	Damage 6	Yes	50 mm	D6
	8	Damage 7	Yes	100 mm	D7
	9	Damage 8	Yes	150 mm	D8
	Run	Structure condition	Damage	Distance from PZT#2 (Direction Disc-2)	Nomenclature /Graphic
PZT#2	10	Damage 9	Yes	Opposed	D9
	11	Damage 10	Yes	10 mm	D10
	12	Damage 11	Yes	20 mm	D11
	13	Damage 12	Yes	30 mm	D12
	14	Damage 13	Yes	40 mm	D12
	15	Damage 14	Yes	50 mm	D14
	16	Damage 15	Yes	100 mm	D15

6. RESULTS

The results were divided into two topics, the first shows the influence of different rotor speed on the impedance signals. And the last shows some results when the rotor was stationary to evaluate the ISHM technique to detect damages.

6.1 Rotor Speed

Temperature variation effects are known to cause horizontal (frequency) and vertical (amplitude) shifts in the impedance signatures. So, a hybrid minimization algorithm was used to compensate the environmental and rotor-operating conditions (temperature and rotating speed), the evolutionary optimizer DE was performed 5 times considering 10 individuals in the initial population (this is one of the advantages of DE). The RMSD damage metric was used as objective function. The impedance signatures were digitally filtered with a 3rd order Savitsky-Golay Finite Impulse Response (FIR) smoothing filter with a frame size of 200. All the data obtained in this experiment are treated with this procedure described.

Figures 6 (a) and 7(a) illustrates the impedance signatures and damage metric under different rotor speed without damage obtained from PZT #1, respectively, before and after using the optimization procedure. The room temperature was 27.67°C ±2.56. Figures 6 (a) and 7(b) shows the impedance signals and damage index after optimization procedure, respectively. Analyzing Fig. 7(b) the damage metric increases in function of the rotor speed.

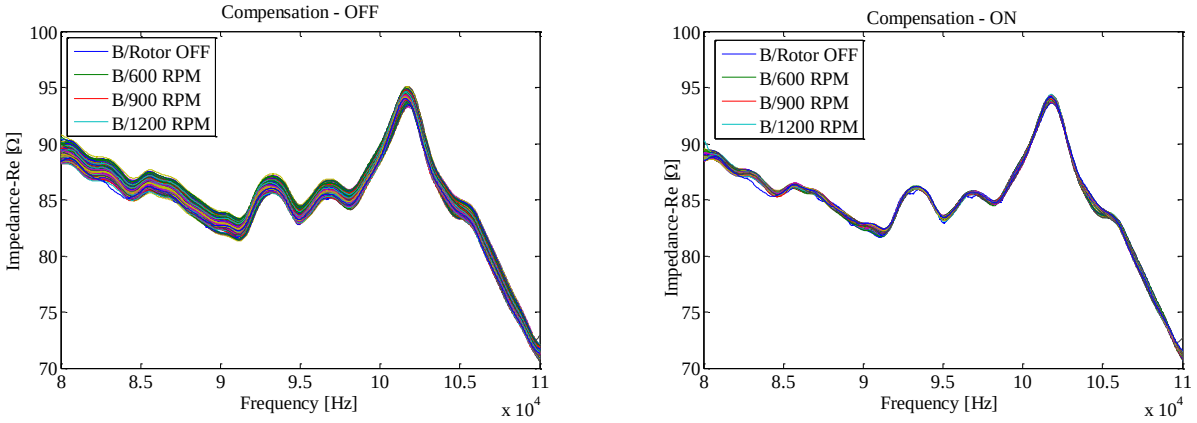

Figure 6 – Impedance signatures (Re) – PZT#1: (a) Temperature and rotor operation conditions on the signature measured by PZT#1 without damage; (b)Temperature and rotor operation conditions with temperature compensation.

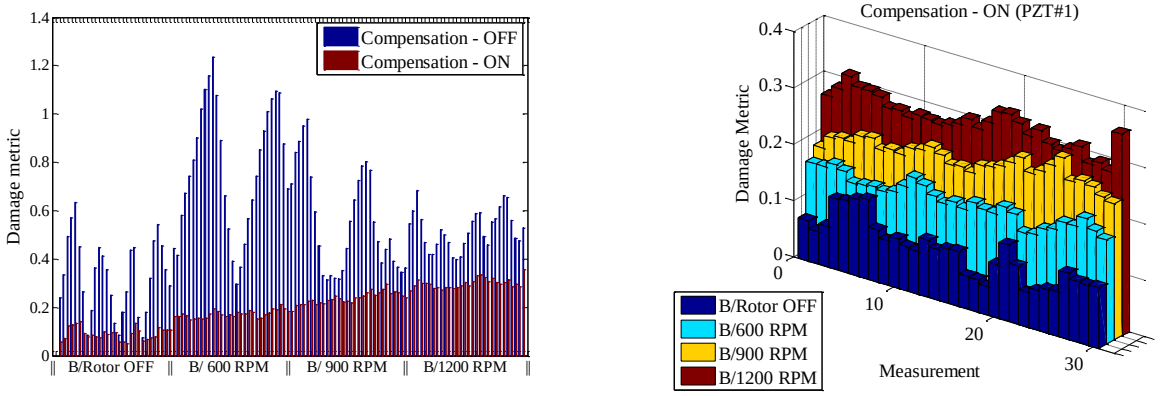

Figure 7 - PZT#1: (a) Temperature compensation effect on damage metric; (b) Impedance signature with compensation ON.

6.2 Damage Detection

Figures 8 and 9 presents the damage metric values of the PZT#1 and PZT #2, respectively. These damages indexes were obtained from the impedance signals applying the compensation procedure. The damage metrics from baseline conditions were used to stablish the statistical threshold with 95,45 % confidence for damage identification according to Eq. 3. Tables 2 and 3 presents the percentage of damage presence in each condition of the PZT #1 and PZT#2, respectively. This percentage was calculated based on the number of RMSD values below the threshold for each run, considering that each one of the had a total of 30 impedance measurements in the frequency range.

For PZT#1, Tab. 2 shows that damages were detected for nearly all measures. At some cases, as in damages 7, 8 and 9, not all values of the metric were above the threshold, but yet the percentage of detection was high, being no less than 90%. In cases like that, we can consider that the method was able to detect damage. However, PZT#2 was not successful in detecting damage for some cases. As seen in Tab. 3, the percentage of detection for damages 4, 5, 6 and 7 was very small or the damage was not detected at all.

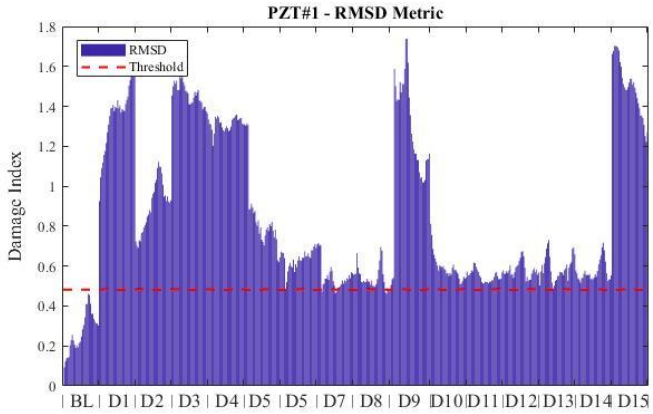

Figure 8. Values of RMSD damage index for PZT#1 with rotor at rest.

Table 2. Global damage detection results (PZT#1).

	Run	Structure condition	Damage	Distance from PZT#1 (Direction Disc-1)	Nomenclature/ Graphic	Damage Detection [%]
PZT#1	1	Baseline	-	-	BL	-
	2	Damage 1	Yes	Opposed	D1	100
	3	Damage 2	Yes	10 mm	D2	100
	4	Damage 3	Yes	20 mm	D3	100
	5	Damage 4	Yes	30 mm	D4	100
	6	Damage 5	Yes	40 mm	D5	100
	7	Damage 6	Yes	50 mm	D6	100
	8	Damage 7	Yes	100 mm	D7	90
	9	Damage 8	Yes	150 mm	D8	90
	10	Damage 9	Yes	300 mm	D9	96,7
	11	Damage 10	Yes	290 mm	D10	100
	12	Damage 11	Yes	280 mm	D11	100
	13	Damage 12	Yes	270 mm	D12	100
	14	Damage 13	Yes	260 mm	D12	100
	15	Damage 14	Yes	250 mm	D14	100
	16	Damage 15	Yes	200 mm	D15	100

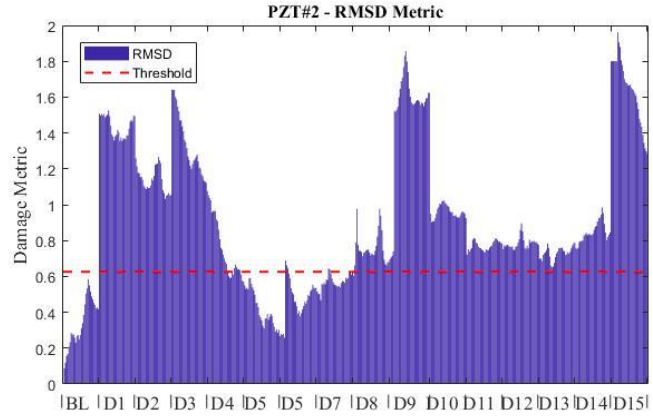

Figure 9. Values of RMSD damage index for PZT#2 with rotor at rest.

Table 3. Global damage detection results (PZT#2).

	Run	Structure condition	Damage	Distance from PZT#2 (Direction Disc-2)	Nomenclature/ Graphic	Damage Detection [%]
PZT#2	10	Damage 9	Yes	Opposed	D9	96,7
	11	Damage 10	Yes	10 mm	D10	100
	12	Damage 11	Yes	20 mm	D11	100
	13	Damage 12	Yes	30 mm	D12	100
	14	Damage 13	Yes	40 mm	D12	100
	15	Damage 14	Yes	50 mm	D14	100
	16	Damage 15	Yes	100 mm	D15	100
	9	Damage 8	Yes	150 mm	D8	100
	8	Damage 7	Yes	200 mm	D7	3,3
	7	Damage 6	Yes	250 mm	D6	3,3
	6	Damage 5	Yes	260 mm	D5	0,0
	5	Damage 4	Yes	270 mm	D4	6,7
	4	Damage 3	Yes	280 mm	D3	100
	3	Damage 2	Yes	290 mm	D2	100
	2	Damage 1	Yes	300 mm	D1	100

7. CONCLUSIONS

The present work analyzed the application of the ISHM method to detect damage in a rotating composite hollow shaft. The ability to detect damage with this technique was investigated for the rotor was turned off, also the influence of different speed rotor was evaluated. For rotor under operation, a hybrid minimization algorithm was applied to reduce temperature and rotating effects on the impedance signal.

For the rotor turned off, PZT#1 was able to detect damage in all cases, but in some cases the detection was not as effective. As shown in Fig. 3, PZT#2 was not able to detect damages 4, 5, 6 and 7, since the values of the damage metric were below the threshold. In general, the hardest damages to detect were the same for both PZTs, showing that they behave similarly. These damages were 7 and 8. In both cases the damages that were better detect were those opposed to the PZTs and the one between then, Damage 9. Both PZTs were able to detect damage in a 150 mm radius. The hybrid minimization algorithm was successful in minimizing the environmental effects and the influence of the operating rotor, as seen in Fig 7.

Further studies will investigate the capability of the damage to detect damage with the operating rotor and the effectiveness of the algorithm to minimize influences with the damaged shaft.

8. ACKNOWLEDGEMENTS

The authors are thankful for the financial support provided to the present research effort by CNPq (574001/2008-5,304546/2018-8, and 431337/2018-7), FAPEMIG (23117.059962/2018-09, TEC-APQ-3076-09, TEC-APQ-02284-15, TEC-APQ-00464-16, and PPM-00187-18), CAPES through the INCT-EIE, and PETROBRAS (5850.0109102.18.9).

9. REFERENCES

Alwan, V., Gupta, A., Sekhar, A. S., Velmurugan, R., 2010. “Dynamic analysis of shafts of composite materials”, *Journal of Reinforced Plastics and Composites*, pp. 2364-2379.

Cavalini Jr, A. A., Finzi Neto, R. M., Steffen Jr, V., 2014. “Impedance-based fault detection methodology for rotating machines”. *Structural Health Monitoring: An International Journal*, vol. 14(3), pp 228–240.

Cavalini Jr, A. A., Guimarães, T. A. M, da Silva, B. R. M. G., Steffen Jr, V., 2017. “Analysis of the Dynamic Behavior of a Rotating Composite Hollow Shaft”, *Latin American Jounal of Solids and Structures*, vol. 14.

Crompton Technology Group Limited. Transmission Shafts. Website: <http://www.ctgltd.com/solutions/transmission-shafts-and-composite-couplings>. Accessed on: January 31th 2019.

Gresil, M, Yu, L., Giurgiutiu, V., Sutton, M., 2012. “Predictive modeling of electromechanical impedance spectroscopy for composite materials”, *Structural Health Monitoring*, vol. 11, pp. 671-683.

Finzi Neto, R. M., Steffen Jr, V., Rade, D. A., 2011. "A low-cost electromechanical impedance-based SHM architecture for multiplexed piezoceramic actuators*." Structural Health Monitoring*, vol. 10, pp. 391–402.

Liang, C., Sun, F.P., Rogers., C.A., 1994. "Coupled Electromechanical Analysis of Adaptive Material Systems – Determination of the Actuator Power Consumption and System Energy Transfer", *Journal of Intelligent Material Systems and Structures*, Vol. 5, pp. 12–20.

Mendonça, W. R. P., de Medeiros, E. C., Pereira, A. L. R., 2017. "Dynamic analysis of rotors mounted on composite shafts with internal damping", *Composite Structures*, vol. 167, pp. 50-62.

Na, S., Lee, H.K., 2012. "Resonant frequency range utilized electro-mechanical impedance method for damage detection performance enhancement on composite structures", *Composite Structures*, vol. 94, pp. 2383-2389.

Palomino, L. V., 2008. *Monitoramente de integridade estrutural de materiais compostos sujeitos a impactos empregando a técnica da impedância eletromecânica*. Master dissertation, Universidade Federal de Uberlândia, Uberlândia, Brazil.

Park, G., Farrar, C. R., di Scalea, F. L., Coccia, S., 2006. "Performance assessment and validation of piezoelectric active-sensors in structural health monitoring", *Smart Materials and Structures*, vol. 15, pp. 1673-1683.

Park, G., Inman, D.J., "Impedance-based structural health monitoring." In: Inman DJ, Farrar CR, Lopes V Jr, *et al*. [Damage prognosis for aerospace, civil and mechanical system]. 1st ed. John Wiley & Sons, Chichester, 1-12 2005.

Peairs D. M., "High Frequency Modeling and Experimental Analysis for Implementation of Impedance-based Structural Health Monitoring" 150 f. *Thesis – Virginia Polytechnic Institute and State University, Virginia.* 2006.

Price, K. V., Storn, R. M., Lampinen, J. A. *"*Differential evolution – a practical approach to global optimization*"*, Springer. Heidelberg, Germany, (2005).

Rabelo D. S., Steffen Jr. V., Finzi Neto R. M., Lacerda H.B., *Impedance-based structural health monitoring and statistical method for threshold-level determination applied to 2024-T3 aluminum panels under varying temperature.* Structural Health Monitoring 1(1): 1-17, 2016.

Schwankl, M., Sharif-Khodaei, Z., Aliabadi, M. H., Weimer, C., 2012. "Electro-Mechanical Impedance Technique for Structural Health Monitoring of Composite Panels". *Key Engineering Materials*, vols. 525-526, pp. 569–572.

Selva, P., Cherrier, O., Budinger, V., Lachaud, F., Morlier, J., 2013. "Smart monitoring of aeronautical composites plates based on electromechanical impedance measurements and artificial neural networks", *Engineering Structures*, vol. 56, pp. 794-804.

Sino, R., Baranger, T. N., Chatelet, E., Jacquet, G., 2008. "Dynamic analysis of a rotating composite shaft", *Composites Science and Technology*, vol. 68, pp. 337-345.

Song, H., Lim, H. J., Sohn, H., 2013. "Electromechanical impedance measurement from large structures using a dual piezoelectric transducer", *Journal of Sound and Vibration*, vol. 332, pp. 6580-6595.

Storn R., Price K., *Differential evolution: a simple and efficient adaptive scheme for global optimization over continuous spaces*. Int.Comp. Sci Inst. 12(1), 1-16, (1995).

Tsuruta, K. M., 2008. *Análise das métricas de dano associadas à técnica da impedância eletromecânica para o monitoramento da integridade estrutural.* Master dissertation, Universidade Federal de Uberlândia, Uberlândia, Brazil.

Tsuruta, K.M., Rabelo, D.S., Guimarães, C.G., Cavalini Jr, A.A., Finzi Neto, R.M., Steffen Jr, V., 2017. "Electromechanical impedance-based fault detection in a rotating machine by using an operating condition compensation approach" In*: SPIE Smart Structures and Materials + Nondestructive Evaluation and Health Monitoring*, Portland, 2017.

Wandowski, T., Malinowski, P.H., Ostachowicz, W.M., 2016. "Delamination detection in CFRP panels using EMI method with temperature compensation", *Composite Strucutures*, vol. 151, pp. 99-107.

Wilson, C. L., Lonkar, K., Roy, S., Kopsaftopoulos, F., Chang, F., 2018. "Structural Health Monitoring of Composites", *Comprehensive Composite Materials II*, vol. 7, pp. 382-407.

10. RESPONSIBILITY NOTICE

The authors are the only responsible for the printed material included in this paper.